Imaging Lipid Distributions in Model Monolayers by ToF-SIMS with Selectively Deuterated Components and Principal Components Analysis

Mark C. Biesinger[1], David J. Miller[1,2], Robert R. Harbottle[2], Fred Possmayer[3], N. Stewart McIntyre[1,2] and Nils O. Petersen[4]

[1]Surface Science Western, The University of Western Ontario, London, Ontario N6A 5B7 Canada
[2]Department of Chemistry, The University of Western Ontario, London, Ontario N6A 5B7 Canada
[3]Department of Obstetrics & Gynecology, The University of Western Ontario, London, Ontario N6A 5B7 Canada
[4]National Institute for Nanotechnology and Department of Chemistry, University of Alberta W6-017 ECERF Bldg, 9107-116th Street, Edmonton, Alberta T6G 2V4 Canada

Abstract

Time of Flight Secondary Ion Mass Spectrometry (ToF-SIMS) provides the capability to image the distribution of molecular ions and their associated fragments that are emitted from monolayer films. ToF-SIMS can be applied to the analysis of monolayers of complex lipid mixtures that act as a model to understand the organization of cell membranes into solid-like domains called lipid rafts. The ability to determine the molecular distribution of lipids using ToF-SIMS in monolayer films is also important in studies of the function of pulmonary surfactant. One of the limitations of the use of ToF-SIMS to studies of complex lipid mixtures found in biological systems, arises from the similarity of the mass fragments that are emitted from the components of the lipid mixture. The use of selectively deuterated components in a mixture overcomes this limitation and results in an unambiguous assignment of specific lipids to particular surface domains. The use of deuterium labeling to identify specific lipids in a multi-component mixture can be done by the deuteration of a single lipid or by the addition of more than one lipid with selectively deuterated components. The incorporation of deuterium into the lipid chains does not alter the miscibility or phase behavior of these systems. The use of deuterium labeling to identify lipids and determine their distribution in monolayer films will be demonstrated using two biological systems. Principal components analysis (PCA) is used to further analyze these deuterated systems checking for the origin of the various mass fragments present.

Keywords: lipid separations, deuterated, labeling, monolayers, principal components analysis (PCA)

1. Introduction

Lipids in model membranes, cell membranes and monolayers of pulmonary surfactants are known to segregate into liquid condensed domains with distinct physical properties and compositions [1-6]. Depending upon temperature and total composition, the domains have liquid-like or solid-like properties and can vary in size over orders of magnitude (50 nm to 50 μm). Importantly, the size, shape and composition of these domains appear to be functionally relevant. In mammalian cell membranes, sub-micron sized, solid-like domains (rafts) enriched in cholesterol and sphingomyelin, are purported to act as signaling complexes [7]. In pulmonary surfactant the lipid organization determines function since micron-sized, solid like domains of fully saturated phospholipid are believed to stabilize pulmonary surfactant at the high surface pressures (low surface tensions) needed to maintain lung function [8-10].

Tools, such as fluorescence microscopy, Brewster angle microscopy and atomic force microscopy allow us to study the sizes and shapes of the phase-segregated domains and, in selected cases, their physical properties. However, none of these tools provide information about the chemical composition of the different phases or of the distribution of specific lipid or protein species among the domains on the surface of a monolayer film or cell membrane. In recent years,

time-of-flight secondary ion mass spectrometry (ToF-SIMS) has provided a novel opportunity to study, with sub-micrometer resolution, the distribution of chemical species across a surface within a depth of 10 – 20Å [11]. TOF-SIMS has successfully been used to study the lipid phase segregation into domains in monolayers of pure and simple mixtures [12-14] and, in one case, of a functional pulmonary surfactant [15]. However, the application of ToF-SIMS and the type of information available has been limited by the fact that most of the phospholipids found in these artificial and natural systems are chemically very similar. The phospholipids all contain fatty acids with fourteen to eighteen carbons, a phosphoglycerol unit and a polar 'head group' such as choline or glycerol. Consequently, the mass spectral fragments are generally similar and there are only a few truly unique ions (generally referred to as daughter ions), other than the parent ions, that unambiguously can be attributed to a single phospholipid species. Since the ionization yield is low at the higher masses, the contrast in the images of the parent ions tend to be poorer. For example, it is impossible to distinguish unambiguously the specific locations of dipalmitoyl phosphatidyl choline (DPPC), palmitoyl oleoyl phosphatidyl choline (POPC) and palmitoyl oleoyl phosphatidyl glycerol (POPG) in mixtures of the three other than by the parent ion. All species share the palmitic acid unit, two share the phosphatidylcholine unit and two share the oleic acid unit. In more complex mixtures, such as in natural systems, the challenge is formidable. Some improvements in the specificity of the SIMS contrast in the lipid and protein films can be gained with tools such as principal components analysis (PCA) [16,17]. Effects due to topography and changes in the matrix are greatly reduced so that the image signal to noise is improved significantly relative to the individual molecular ion images of the parent ions and major fragment peaks.

Recently, ToF-SIMS studies with deuterated species have shown that the deuterium tracer yields specific mass peaks, that can be studied using the imaging mode ToF-SIMS, to produce superior information about the organization of specific molecular species in a film [18,19]. These studies have been limited to proteins and ions so far but the principle can be applied to studies of lipid organization as well.

In this study, we show that by using selectively deuterated phospholipids, ToF-SIMS provides unambiguous measurements of the distribution of a specific phospholipid in a representative deposit of a mixed lipid monolayer. The approach alleviates concerns about distributions of fluorescent tracers (e.g. exclusion of the NBD-PE from the liquid condensed phases) since the chemical perturbation induced by deuterium incorporation is minimal. The results point to two general strategies for studying the distribution of composition in a mixed monolayer (or bilayers): first, mixing of differently labeled deuterated phospholipids that provide unique mass markers for each species; and second, introduction of a single, deuterated species as a tracer, to be mapped on the sample surface at high sensitivity through the unique mass of the D^- ion at a mass of two. Principal components analysis (PCA) is applied to these imaging datasets demonstrating that the combination of the two techniques allow for the elucidation of information not readily observable in the ToF-SIMS images alone, particularly components present at low concentrations.

2. Experimental

2.1 Materials

All lipids used were purchased from Avanti Polar Lipids (Alabaster), and were received in $CHCl_3$. Samples were diluted to 1 mg/ml and stored at –20 °C until use. Purity and identity of all the lipids were checked using electrospray ionization mass spectrometry and were found to be within Avanti specifications. All solvents used in cleaning and in dilutions were of HPLC grade and were used without further purification.

2.2 Langmuir-Blodgett Films of 5:3:2 DPPC-d_4:POPC:POPG-d_{31}

Langmuir-Blodgett (LB) films of mixtures of (5:3:2 molar ratio) dipalmitoyl phosphatidyl tetradeuterocholine (DPPC-d_4), where the four deuterons are in the methylenes of the choline group ($-O-CD_2CD_2-N^+(CH_3)_3$), palmitoyl oleoyl phosphatidyl choline (POPC), and perdeuteropalmitoyl

oleoyl phosphatidyl glycerol (POPG-d_{31}) were prepared. Lipid monolayers were spread from a chloroform solution onto doubly distilled water in a μ-trough SE Langmuir balance (Kibron, Helsinki, Finland). The film was compressed at a rate of 0.04 nm^2 $molecule^{-1}$ min^{-1} at ambient temperatures and a monitored pH of 7.0 ±0.5 until the desired pressure of 40 mN/m was reached. The monolayer film was deposited onto gold-coated mica by elevating the previously submerged mica vertically through the air-water interface at a rate of 2.0 mm/min. The monolayers were equalized for constant pressure during deposition. The transferred films used in this study have transfer ratios of approximately unity (i.e. monomolecular films). The substrate was prepared as described earlier [1] by sputtering gold onto freshly cleaved mica under vacuum in a Hummer VI sputtering system (Technics EMS Inc. Springfield, VA) for 6 minutes at a plate current of 10 mA.

Monolayer films such as this have been shown to separate into two distinct regions, a liquid expanded (LE) phase, in which the hydrocarbon tails are fluid, and a liquid condensed (LC) phase, in which the tails are more rigid [20]. These features are readily discernible in the ToF-SIMS images.

2.3 Langmuir-Blodgett Films of Cholesterol-d_7 (2 mol.%) and DPPC

Langmuir-Blodgett (LB) films of mixtures of a 2 mol % cholesterol-d_7 in dipalmitoyl phosphatidyl choline (DPPC) were prepared with trough conditions similar to that for the films of 5:3:2 DPPC-d_4:POPC:POPG-d_{31} described above (section 2.2). Cholesterol-d_7 has seven deuterons at the end of the hydrocarbon tail off the ring structure (-$CD(CD_3)_2$).

2.4 TOF-SIMS Imaging Conditions

ToF-SIMS images were collected using an ION-TOF TOF-SIMS IV (ION-TOF GmbH, Munster, Germany) with a 25 keV gallium ion primary ion beam in "burst alignment" or medium-current mode. This mode uses a pulse width of 200 ns, spot size in the 250 nm range, and mass resolution of $M/\Delta M = 300$. All images obtained were 256 x 256 pixels. From previous studies [16] it is known that the static limit for these materials is passed at approximately 8 x 10^{12} ions/cm^2. Generally, an ion dose of 5 x10^{12} ions/cm^2 was not exceeded for these analyses (equivalent to approximately 10 scans for a 100 x 100 μm image at 1 pA primary ion current and 3 scans for a 50 x 50 μm image at 1 pA).

2.5 PCA Software

PLS_Toolbox 2.1 from Eigenvector Research running on Matlab 6.0 was the software used for PCA analysis. For each set of data as many significant mass peaks as possible were added to the peak list for analysis. For example, in the case of the 5:3:2 DPPC-d_4 : POPC : POPG-d_{31} study, more than 130 are selected. Also included in the peak selection is the total remaining ion image (sum of ion intensity not selected as a specific peak) shown at mass zero in the loadings. This image is usually significant in that it contains a significant amount of topographic and matrix information. A conversion routine transforms the ToF-SIMS data (saved as a binary file) into a matrix usable by the PLS_Toolbox software. The data are then unfolded so that an image that was originally *I* by *J* pixels with *K* spectral channels is reshaped to form a 2-D array that is *I*J* by *K*. All data was "autoscaled" prior to PCA. In this procedure, the data are first mean-centered. This is done by subtracting the column mean from each column, thus forming a matrix where each column has a mean of zero. Each mean-centered variable is then divided by its standard deviation, which results in variables with unit variance. This procedure puts all variables on an equal basis in the analysis. Thus, the less intense but more chemically significant higher mass peaks receive the same level of consideration in the analysis as the intense, low mass peaks. The principal components analysis model is then applied to the data. After scores have been calculated for each pixel, the pixels are reorganized to the original image dimensions (*I* by *J*) and displayed as pseudocolor maps. This gives a graphic representation of the score value of each pixel as a function of position. Examination of the corresponding loadings for each score image gives information about the various spectral variables (mass fragments) that are correlated with that score image.

3. Results and Discussion

3.1 Langmuir-Blodgett Films of 5:3:2 DPPC-d_4:POPC:POPG-d_{31} (Positive Ion Images)

With sufficient amounts of each phospholipid and deuteration of appropriate components the individual positive ion ToF-SIMS images (Figure 1) of selected masses for this system very nicely show(s) the distribution of the three phospholipids. Deuterated long chain hydrocarbon fragments such as masses 30 (C_2D_3), 34 (C_2D_5), 46 (C_3D_5), 50 (C_3D_7), 62 (C_4D_7), and 66 (C_4D_9) clearly show POPG-d_{31} to be within the liquid expanded (LE) phase. Also present in the LE phase are undeuterated mass fragments such as 72 ($C_4H_{10}N$), 86 ($C_5H_{12}N$), 104 ($C_5H_{13}NOH$), 166 ($C_5H_{13}NPO_3$, phosphocholine – H_2O), and 184 ($C_5H_{13}NPO_4H_2$, phosphocholine) attributed to POPC. Within the liquid condensed (LC) phase, the deuterated components of the phosphocholine in DPPC-d_4 are found. Specifically, peaks at mass 76 ($C_4H_8D_3N$), 89 ($C_5H_9D_3N$), 108 ($C_5H_9D_4NOH$), 170 ($C_5H_9D_4NPO_3$) and 188 ($C_5H_9D_4NPO_4H_2$) are important.

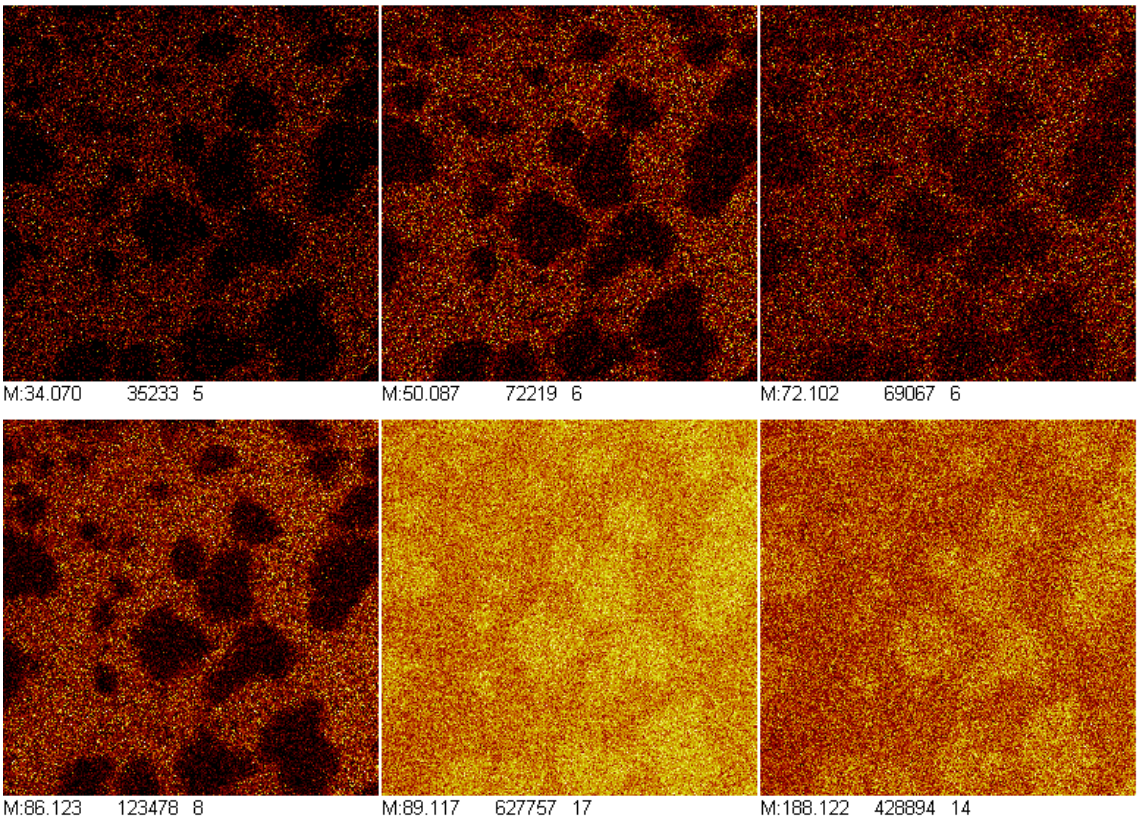

Figure 1. Selected ToF-SIMS positive ion images from an LB film of 5:3:2 DPPC-d_4:POPC:POPG-d_{31}. Images are 100x100 μm. Clockwise from top left, masses 34 (C_2D_5) and 50 (C_3D_7) representing POPG-d_{31}, masses 72 ($C_4H_{10}N$) and 86 ($C_5H_{12}N$) representing POPC, and masses 89 ($C_5H_9D_3N$) and 188 ($C_5H_9D_4NPO_4H_2$) representing DPPC-d_4.

The first two image scores from the principal components analysis (PCA) of this system are shown in Figure 2. Principal component 1 (PC 1) gives a very clear image of the two phases in this system. This image is stronger and clearer than any of the individual TOF-SIMS images obtained. PC 2 shows only the effect of some topography manifested as a slight tilt to the sample. Returning to PC 1, positive loadings, represented graphically in Figure 3 and partially tabulated in Table 1, will corresponds to mass fragments that are found in the LC phase. The more positive the loading the stronger the correlation is. Alternately, negative loadings will correspond to mass fragments found in the LE phase. Mass fragments having only a slightly positive or slightly negative loading

are likely spread throughout both phases. Inspection of the table clearly shows the DPPC-d_4 in the LC phase with the POPC and POPG-d_{31} in the LE phase. Mass fragments common to both phases (such as D and palmitate) will have lower loading scores. Interestingly, undeuterated hydrocarbon fragments (C_xH_y), common to both DPPC-d_4 and POPC, load positively with other DPPC-d_4 fragments. This is due to two factors: 1) the fact that DPPC-d_4 is present in larger quantities than POPC (5:3 DPPC-d_4:POPC) and 2) the orientation of DPPC-d_4 (ordered in the LC phase) compared to POPC (disordered in the LE phase). The hydrocarbon tails of DPPC-d_4 are vertical and as such hydrocarbon fragments will be seen in greater amount than the corresponding head-group of the molecule. The surface density of DPPC-d_4 is also slightly greater in the LC phase than the POPC in the LE phase. In the LE phase, the head-groups of the POPC are more easily accessible and thus will be enhanced compared to the hydrocarbon tails of that molecule. This effect will also be important in the following case with DPPC and cholesterol.

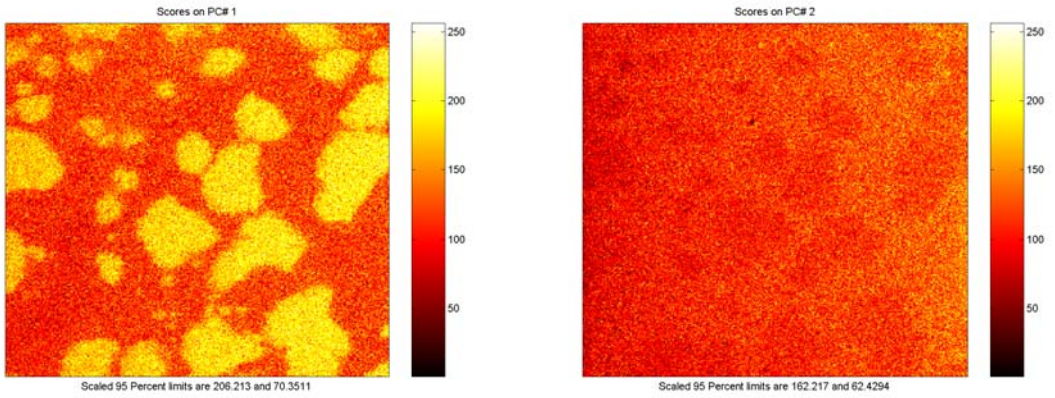

Figure 2. Image scores for PC 1 (left) and PC 2 (right) for an LB film of 5:3:2 DPPC-d_4:POPC:POPG-d_{31} (positive ion images). Image is 100x100 μm.

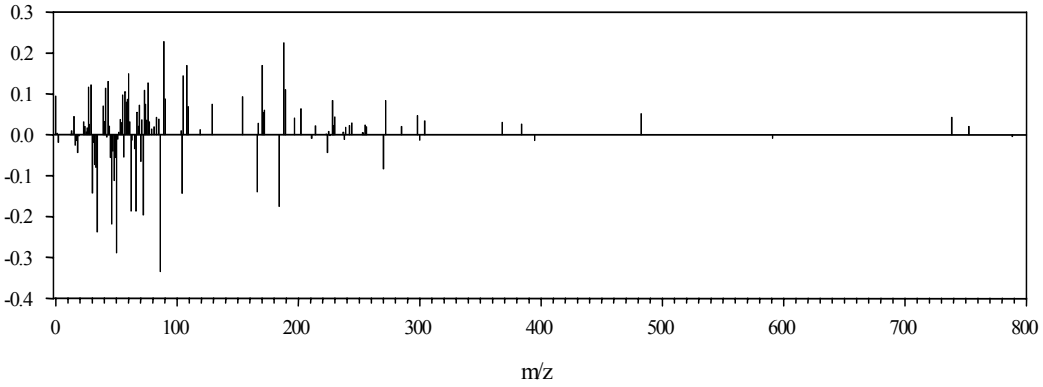

Figure 3. Loadings for PC 1 for an LB film of 5:3:2 DPPC-d_4:POPC:POPG-d_{31} (positive ion images). A positive loading corresponds to the bright areas in the images score (Figure 2–PC 1) representing the LC phase. The negative loadings correspond to the darker areas representing the LE phase.

Mass	Species	Loading	Notes
86	$C_5H_{12}N$	-0.33	POPC
50	C_3D_7	-0.29	POPG-d_{31}
34	C_2D_5	-0.24	POPG-d_{31}
46	C_3D_5	-0.22	POPG-d_{31}
72	$C_4H_{10}N$	-0.20	POPC
66	C_4D_9	-0.19	POPG-d_{31}
62	C_4D_7	-0.19	POPG-d_{31}
184	$C_5H_{13}NPO_4H_2$	-0.17	POPC, phosphocholine
104	$C_5H_{13}NOH$	-0.14	POPC -choline
30	C_2D_3	-0.14	POPG-d_{31}
166	$C_5H_{13}NPO_3$	-0.14	POPC, phosphocholine $-H_2O$
48	C_3D_6	-0.11	POPG-d_{31}
18	CD_3, NH_4	-0.04	POPG-d_{31}, DPPC-d_4
16	CD_2	-0.02	POPG-d_{31}
2	D, H_2	-0.02	POPG-d_{31} and DPPC-d_4, low loading - D found in both phases, H_2 contribution makes mass 2 less useful
255		0.02	Palmitate in both DPPC-d_4 and POPC
739	DPPCd_4 +H	0.04	DPPC-d4, parent +H
55	C_4H_7	0.10	Long chain portion of DDPC-d_4
41	C_3H_5	0.11	Long chain portion of DDPC-d_4
27	C_2H_3	0.12	Long chain portion of DDPC-d_4
29	C_2H_5	0.12	Long chain portion of DDPC-d_4
76	$C_4H_8D_3N$	0.13	DPPC-d_4
43	C_3H_7	0.13	Long chain portion of DDPC-d_4
105		0.14	DDPC-d_4 - not fully deuterated fragment
60		0.15	DDPC-d_4 - not fully deuterated fragment
170	$C_5H_9D_4NPO_3$	0.17	DPPC-d_4
108	$C_5H_9D_4NOH$	0.17	DPPC-d_4
188	$C_5H_9D_4NPO_4H_2$	0.22	DPPC-d_4
89	$C_5H_9D_3N$	0.23	DPPC-d_4

Table 1. Selected species of interest and their loadings for PC 1 for an LB film of 5:3:2 DPPC-d_4:POPC:POPG-d_{31} (positive ion images). A positive loading suggests that species is in the LC phase and a negative loading suggests it is in the LE phase.

3.2 Langmuir-Blodgett Films of 5:3:2 DPPC-d_4:POPC:POPG-d_{31} (Negative Ion Images)

The negative ion ToF-SIMS images (Figure 4), although showing the LC and LE phases, are less useful for determining chemical compositions in this system. Strong images include deuterium, phosphate fragments (PO_3, PO_3H, PO_4, PO_4H, PO_4H_2), oleate from POPC (masses 286, 287), and the palmitate from DPPC and POPC. However, information of interest in this and other systems may be found when this data is taken in conjunction with the positive ion images obtained.

PCA analysis of the negative ion images again gives a strong image score for PC 1 showing the distribution of LC and LE phases (Figure 5). PC 2 is almost insignificant, showing only a small dark area attributable to a small pit in the substrate surface. Loadings for PC1, shown in Figure 6 with selected ions tabulated in Table 2, show that deuterium, short deuterated fragments and the oleate are dominate in the LE phase while the total remaining ion image and phosphate fragments dominate species the LC phase.

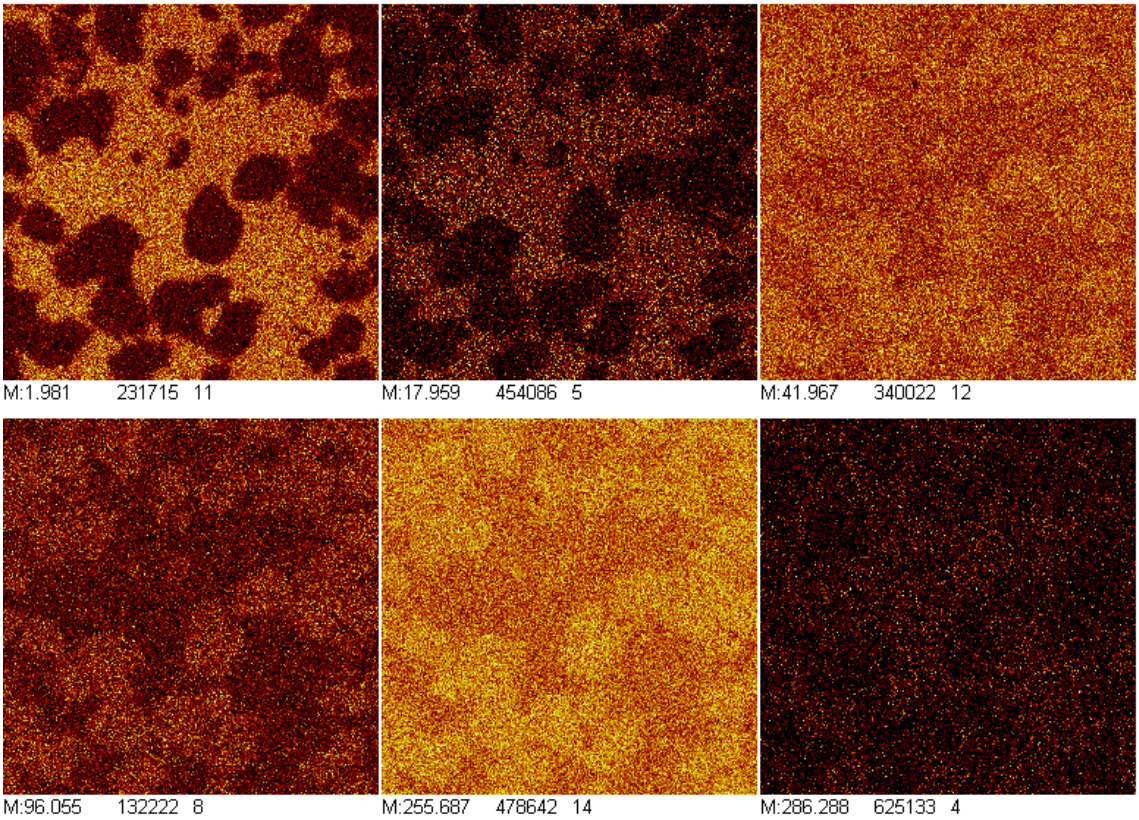

Figure 4. Selected ToF-SIMS negative ion images from an LB film of 5:3:2 DPPC-d_4:POPC:POPG-d_{31}. Images are 100x100 μm. Clockwise from top left, masses 2 (D), 18 (CD_3), 42 (CNO), 96 (PO_4), 255 (palmitate), and 286 (perdeuteroplamitate from POPG-d_{31}).

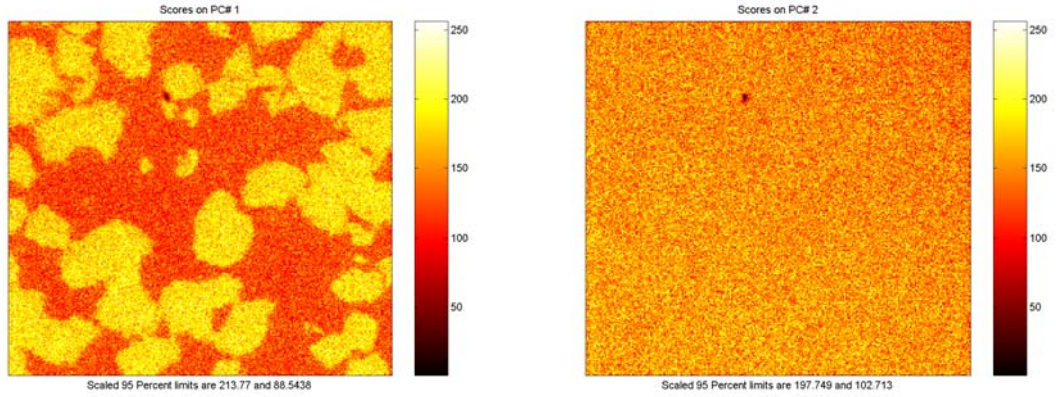

Figure 5. Image scores for PC 1 (left) and PC 2 (right) for an LB film of 5:3:2 DPPC-d_4:POPC:POPG-d_{31} (negative ion images). Image is 100x100 μm.

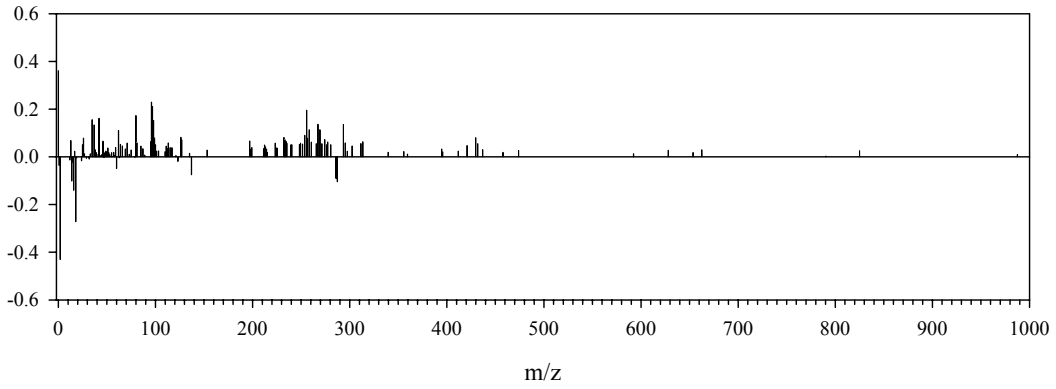

Figure 6. Loadings for PC 1 for an LB film of 5:3:2 DPPC-d_4:POPC:POPG-d_{31} (negative ion images). A positive loading corresponds the bright areas in the images score (Figure 5–PC 1) representing the LC phase. The negative loadings correspond to the darker areas representing the LE phase.

Mass	Species	Loading	Notes
2	D	-0.43	D mostly from POPG-d_{31}
18	CD_3	-0.27	Deuterated fragment from POPG-d_{31}
16	CD_2, O	-0.14	
287		-0.11	Oleate from POPC
14	CD, CH_2	-0.10	
286		-0.09	Perdeuteropalmitate from POPG-d_{31}
1	H	-0.04	
15	CH_3	-0.02	
24	C_2	-0.02	
12	C	-0.01	
26	C_2H_2, C_2D	0.08	
99	PO_4H_3	0.08	
37	C_3H, ^{37}Cl	0.13	
98	PO_4H_2	0.15	
35	Cl	0.16	
42	CNO	0.16	
80	PO_3H	0.17	
256		0.19	Palmitate from DPPC-d_4 (much stronger then that from POPC)
97	PO_4H	0.21	
96	PO_4	0.23	
0		0.36	Total remaining ions

Table 2. Selected species of interest and their loadings for PC 1 for an LB film of 5:3:2 DPPC-d_4:POPC:POPG-d_{31} (negative ion images). A positive loading suggests that species is in the LC phase and a negative loading suggests it is in the LE phase.

3.3 Langmuir-Blodgett Films of Cholesterol–d_7 (2 mol.%) and DPPC (Positive Ion Images)

Of the ion images taken before reaching the static limit for this system very few show the spiral LC phases with sufficient strength as to be useful. Figure 7 shows the strongest of these, masses 86 and 104 along with mass 18, a possible deuterated fragment (CD_3), although it could also be that from NH_4 or H_2O. Also shown are these same masses from images that have been collected with an ion flux of approximately twelve times the static limit. None of the pre-static limit images (nor any long scan images) give an indication of the position of the cholesterol-d_7.

PCA analysis of this system again gives a stronger, cleaner image (PC 1) of the LC and LE phases than any of the individual pre-static limit ion images. Ion images taken from long scan times do give excellent images (see Figure 7) but chemical interpretation from these images are compromised. As well, previous studies [16] have shown that after the static limit is surpassed, the contrast of specific images can completely reverse. PC 2 again only shows a minor amount of what are likely slight topographic changes in the substrate surface. Loadings for PC 1 (Figure 8 and selected ion loadings in Table 3) for this system are much more difficult to interpret. This system behaves mostly like a single component system where the differences seen are due to the differing physical states of the lipids in the two phases. Chemical changes, due to the low amount of cholesterol-d_7, are difficult to ascertain. The parent peak of cholesterol-d_7 (mass 393) is not observed and mass 2, in this low mass resolution/high imaging resolution mode, is likely a combination of D and H_2 (positive ion mode).

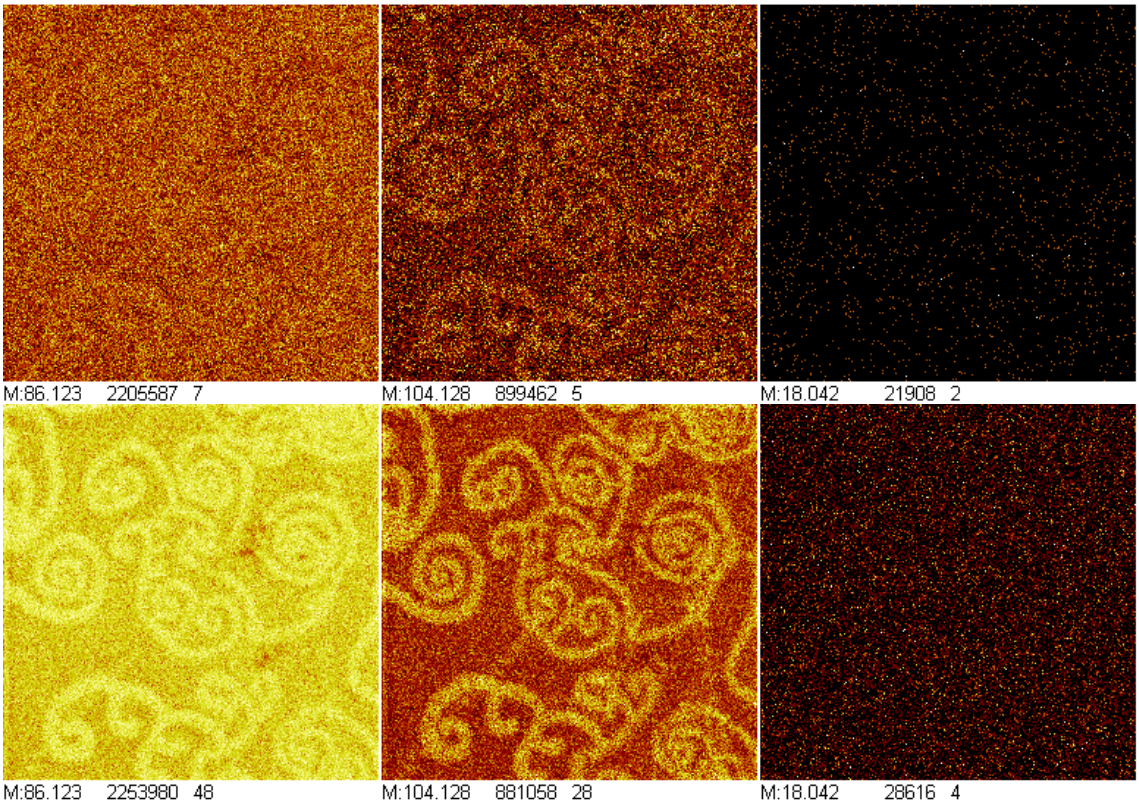

Figure 7. Selected ToF-SIMS positive ion images from an LB film of cholesterol-d_7 (2 mol %) and DPPC. Images are 56x56 μm. Top left to right, masses 86, 104 and 18 of images collected under the static limit. Bottom left to right, same masses collected with ion fluxes 12 times that of the static limit.

Using reference spectra of DPPC and cholesterol-d_7, in conjunction with the PCA results, evidence for the placement of the cholesterol-d_7 in the liquid expanded phase starts to become apparent. Mass fragments consistent with cholesterol-d_7, with image distributions that are undistinguishable in

their individual ion images, have positive loadings for PC 1 – indicative of the LE phase. Strong peaks in the cholesterol-d_7 spectrum include, masses 30, 41, 50, 55, 91, 95, 105 107, 255, 376. Looking at their respective loadings we see that most of these are positive. Of those that are negative explanations can be made. Mass 41, although strong in the spectrum for cholesterol-d_7, is very strong in the DPPC spectrum and is therefore likely to load with that fragment from DPPC, this is similar for other fragments such as those at masses 184, 211, 213, 215, 225, 226 and 255 that are seen in both spectra. The other standout, mass 105, is likely due to the influence of ^{13}C containing $C_5H_{14}NO$ (normally at mass 104) fragment from DPPC. This is the strongest negative loading fragment.

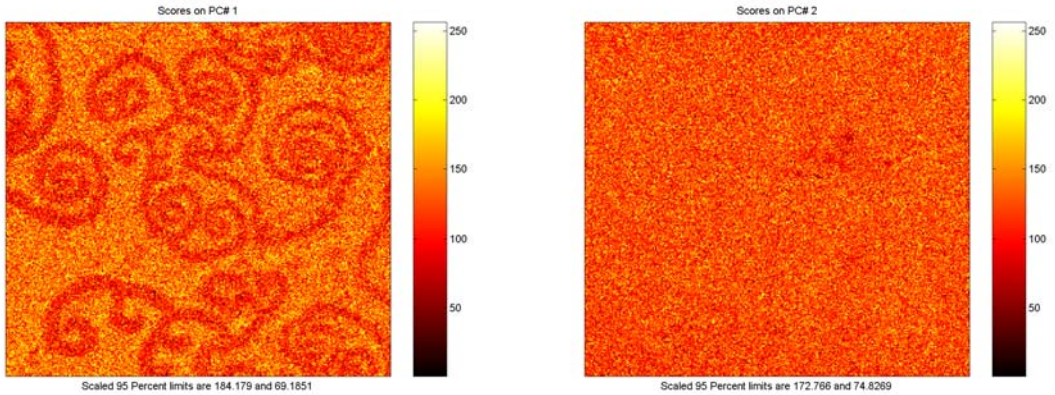

Figure 8. Image scores for PC 1 (left) and PC 2 (right) for an LB film of cholesterol-d_7 (2 mol %) and DPPC (positive ion images) where images are collected under the static limit (see Figure 7 top three images). Images are 56x56 μm.

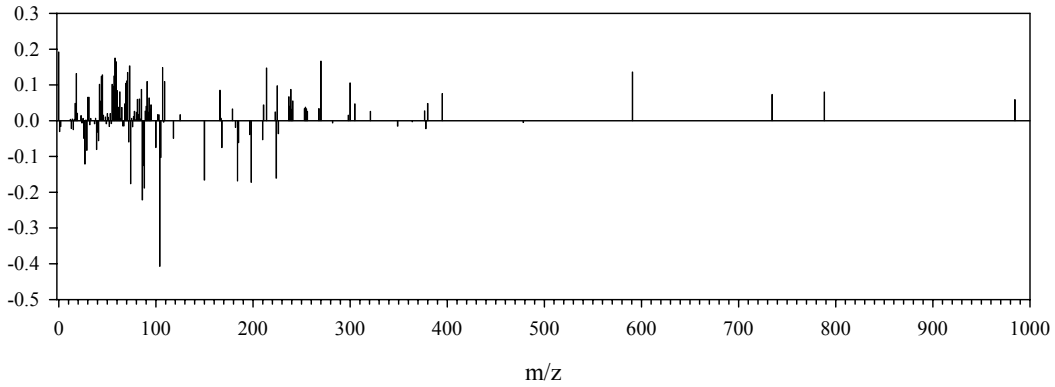

Figure 9. Loadings for PC 1 for an LB film of cholesterol-d_7 (2 mol %) and DPPC (positive ion images). A positive loading corresponds the bright areas in the images score (Figure 8–PC 1) representing the LE phase. The negative loadings correspond to the darker areas representing the LC phase.

Mass	Species	Loading	Notes
104	$C_5H_{14}NO$	-0.41	DPPC fragment
86	$C_5H_{12}N$	-0.22	DPPC fragment
88	$C_5H_{12}O$	-0.19	DPPC fragment
74	$C_4H_{12}N$	-0.18	DPPC fragment
198	Au+H?	-0.17	
184	$C_5H_{15}NPO_4$	-0.17	Cholesterol-d_7 fragment and DPPC fragment
150		-0.17	DPPC fragment
224		**-0.16**	**Cholesterol-d_7 fragment and DPPC fragment**
27	C_2H_3	-0.12	
105		**-0.10**	**$C_5H_{14}NO$ with one ^{13}C and Cholesterol-d_7 fragment**
29	C_2H_5	-0.08	
168		-0.08	DDPC fragment
185		-0.06	DPPC fragment
41	**C_3H_5**	**-0.06**	**Cholesterol-d_7 fragment and DPPC fragment**
197	Au	-0.04	
226		**-0.04**	**Overlap with DPPC**
1	H	-0.03	
15	CH_3	-0.03	
13	CH	-0.02	
2	**D, H_2**	**-0.02**	**Will be mostly H_2 in positive ion mode**
50	**$(CD_3)_2CD$**	**0.02**	**Strong in cholesterol-d_7 spectrum**
376.8		**0.03**	**Cholesterol-d_7 - OH**
255		**0.03**	**Cholesterol-d_7 fragment and DPPC fragment**
95		**0.04**	**Strong in cholesterol-d_7 spectrum**
380		0.05	DDPC fragment
17	CD_2H, OH	0.05	
43	C_3H_7	0.05	
93		**0.06**	**Strong in cholesterol-d_7 spectrum**
31	P, CH_3O	0.07	
30	**CD_3C**	**0.07**	**Strong in cholesterol-d_7 spectrum**
734.6	DPPC parent	0.07	
55	**C_4H_7**	**0.10**	**Strong in cholesterol-d_7 spectrum**
91	**C_7H_7**	**0.11**	**Strong in cholesterol-d_7 spectrum**
57	C_4H_9	0.13	
18	CD_3, H_2O, NH4	0.13	Possible cholesterol-d_7, other species possible
591		0.14	DPPC fragment
214		0.15	DPPC fragment
107		**0.15**	**Strong in cholesterol-d_7 spectrum**
73		0.15	
59		0.17	DPPC fragment
270		0.17	DPPC fragment
58		0.17	DPPC fragment
0		0.19	Total remaining ions

Table 3. Selected species of interest and there loadings for PC 1 for an LB film of cholesterol-d_7 (2 mol %) and DPPC (positive ion images). A positive loading suggests that species is in the LC phase and a negative loading suggests it is in the LE phase. Masses of interest are in bold.

4. CONCLUSIONS

This work has shown that with creative deuterium labeling of specific species within a system that would normally contain species with similar mass fragments, identification and location by ToF-SIMS imaging can be achieved. For samples containing large concentrations of all species of interest, such as those for the LB films of 5:3:2 DPPC-d_4:POPC:POPG-d_{31}, deuterium labeling alone is sufficient for identification of species within specific phases. For this system, principal components analysis (PCA) can still provide useful information as well as producing an image score free of topographic effects and of excellent contrast and resolution compared to most (if not all) ion specific images.

For systems where a minor component is sought (cholesterol-d_7 (2 mol %) and DPPC), deuterium labeling is insufficient. This is especially true where smaller structures demand higher magnification and conversely shorter scan times to remain below the static limit. In this case, labeling in conjunction with PCA can give vital clues as to the location of these minor components. One must however be extremely careful with the interpretation of these results as overlaps of mass fragments, the ratio of components, and strength of mass peaks within a spectrum must all be considered during interpretation.

Other points that need to be carefully considered include instruments settings, particularly the trade-off between high resolution imaging with lower resolution spectroscopy, and the need to remain below the static limit, which can cause considerable loss of signal at higher magnifications.

Acknowledgements

The authors would like to thank Dr. James Francis at Surface Science Western for his help with the TOF-SIMS software and Ms. Nora Keating with her help in locating mass spectra. An NSERC Collaborative Health Research Program Grant and a CIHR Operating Grant supported this work.

References

[1] K. Nag, J.S. Pao, R.R. Harbottle, F. Possmayer, N.O. Petersen, L.A. Bagotolli, Biophys. J. 82 (2002) 2041.
[2] J. Fantini, Cell Mol. Life Sci. 60 (2003) 1027.
[3] K. Nag, J. Perez-Gil, M.L.F. Ruano, L.A.D. Worthman, J. Stewart, C. Casals, K.M.W. Keough, Biophys. J. 74 (1998) 2983.
[4] B. Discher, W.R. Schief, V. Vogel, S. Hall, Biophys. J. 77 (1999) 2051.
[5] D.Y. Takamoto, M.M. Lipp, A. von Nahmen, K.Y.C. Lee, A.J. Waring, J.A. Zasadzinski, Biophys. J. 81 (2001) 153.
[6] M. Amrein, A. von Nahmen, M. Sieber, Eur. Biophys. J. 26 (1997) 349.
[7] T. Harder, P. Scheiffele, P. Verkade, K.J. Simons, Cell Biol. 18 (1998) 929.
[8] R.H. Notter, Z.D. Wang, Rev. Chem. Eng. 13 (1997) 1.
[9] J. Goerke, Biochim. Biophys. Acta. 79 (1998) 1408.
[10] B.M. Discher, K.M. Maloney, D.W. Grainger, C.A. Sousa, S.B. Hall, Biochemistry 38 (1999) 374.
[11] A.M. Belu, D.J. Graham, D.G. Castner, Biomaterials 24 (2003) 3635.
[12] K.M. Leufgen, H. Rulle, A. Benninghoven, M. Sieber, H.-J. Galla, Langmuir 12 (1996) 1708.
[13] N. Bourdos, F. Kollmer, A. Benninghoven, M. Sieber, H.-J. Galla, Langmuir 16 (2000) 1481.
[14] M. Ross, C. Steinem, H.-J. Galla, A. Janshoff, Langmuir 17 (2001) 2437.
[15] R.R. Harbottle, K. Nag, N.S. McIntyre, F. Possmayer, N.O. Petersen, Langmuir 19 (2003) 3698.

[16] M.C. Biesinger, P.-Y. Paepegaey, N.S. McIntyre, R.R. Harbottle, N.O. Petersen, Anal. Chem. 74 (2002) 5711.
[17] J.B. Lhoest, M.S. Wagner, C.D. Tidwell, D.G. Castner, J. Biomed. Mater. Res. 57 (2001) 432.
[18] A.M. Belu, Z. Yang, R. Aslami, A. Chilkoti, Anal. Chem. 73 (2001) 143.
[19] J.B. Cliff, D.J. Gaspar, P.J. Bottomley, D.D. Myrold, Appl. Environ. Microbiol. 68 (2002) 4067.
[20] O. Albrecht, H. Gruler, E. Sackmann, J. Phys. (Paris) 39 (1978) 301.